

Ignition and Combustion Characteristics of Nanoaluminum with Copper Oxide Nanoparticles of Differing Oxidation State

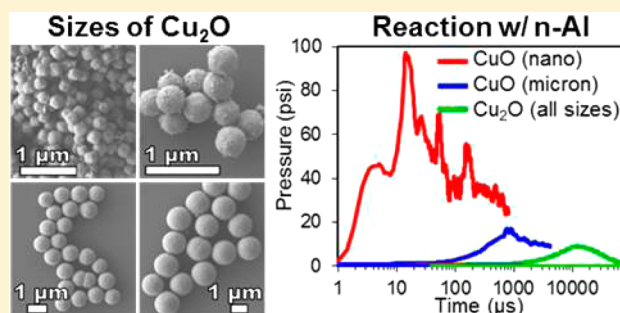
Garth C. Egan,^{†,§} Kyle T. Sullivan,[‡] Tammy Y. Olson,[‡] T. Yong-Jin Han,[‡] Marcus A. Worsley,[‡] and Michael R. Zachariah^{*,†,§}

[†]Department of Chemical and Biomolecular Engineering and Department of Chemistry and Biochemistry, University of Maryland, College Park, Maryland 20742, United States

[‡]Materials Science Division, Lawrence Livermore National Laboratory, Livermore, California 94550, United States

S Supporting Information

ABSTRACT: The importance of the oxidation state of an oxidizer and its impact on gaseous oxygen and total gas production in nanocomposite thermite combustion was investigated by probing the reaction and ignition properties of aluminum nanoparticles (Al-NPs) with both cupric oxide (CuO) and cuprous oxide (Cu₂O) nanoparticles. The gas release and ignition behavior of these materials were tested with >10⁵ K/s temperature jump (T-jump) heating pulses in a high temporal resolution time-of-flight mass spectrometer (ToF-MS) as well as in an argon environment. Reactivity was tested using a constant volume combustion cell with simultaneous pressure and optical measurements. A variety of Cu₂O particle sizes ranging from 200 to 1500 nm were synthesized and found to release oxygen at ~1200 K, which is higher than the values found for a variety of CuO particle sizes (~1000 K). Both oxides were found to ignite around 1000 K, which implies a consistent ignition mechanism for both through a condensed phase pathway. The higher oxidation state (CuO) thermites were found to react faster and produce higher pressures by several orders of magnitude, which implies that gaseous species play a critical role in the combustion process. Differences in reactivity between argon and vacuum environments and the use of Cu diluent to simulate Cu₂O suggest that it is the intermediate product gas, O₂, that plays the most significant role in combustion as an enabler of heat transfer and a secondary oxidizer. The lack of any oxidizer size dependence on ignition is suggestive of rapid sintering that wipes out the effect of enhanced interfacial contact area for smaller oxidizers.



INTRODUCTION

Energetic materials are one of the many areas of research that have seen remarkable gains with the emergence of nanoscale materials and technologies. In particular, the reactivity of thermites, which are highly exothermic mixtures of metal oxide oxidizers and metal fuels, has been increased by several orders of magnitude up to flame speeds of ~1000 m/s through the use of nanoparticles.¹ This increase is generally thought to result from reduced transport distances and increased specific surface areas of nanoscale materials. However, the rapid kinetics, high temperatures, dynamic morphologies, and multiphase nature of these systems have limited our understanding of the mechanisms that control combustion. As a result, there are still many questions that remain about these systems including how choice of oxidizer affects the reaction process.

Generally, it has been shown that systems which produce a significant amount of gaseous species perform best in terms of reactivity.^{2–7} These gases are thought to play a critical role in heat transfer by enabling convection/advection with high pressure gradients that drive hot gases and materials into the cold unreacted zone.^{7–10} In thermites, intermediate gaseous species can originate from the decomposition or sublimation of

the metal oxide and its suboxides. Later-time gases form as the reaction proceeds to completion and produces some fraction of volatile products. Exactly when intermediate and product gases form in respect to the overall reaction process and how they contribute to a propagating reaction are still unknown, as probing these materials dynamically with sufficient spatial and time resolution can be challenging. The exact nature of these gases will also be dependent on the oxidizer used, as there are a wide variety of gas-generating oxidizers which have different sizes, morphologies, decomposition pathways, densities, and enthalpies of formation. Directly comparing two oxidizers is complicated when one accounts for all of these parameters. For this reason, a recently developed method for synthesizing monodisperse Cu₂O over a wide range of sizes¹¹ presents a unique opportunity for studying the chemistry and mechanism behind thermite reaction. By comparing this oxidizer to the higher oxidation state material, CuO, we can compare two systems where the constituent atoms and thus the thermody-

Received: November 7, 2016

Revised: November 18, 2016

Published: November 21, 2016

namics of the final products are the same for both. Further, by testing the material over a wide range of sizes, it will be possible to elucidate the contribution of the oxidizer's size to ignition and combustion. Accounting for that effect then enables determination of how the fundamental properties of an oxidizer, particularly gas production, impact nanocomposite thermite reaction and propagation.

Although CuO–Al has almost twice the specific energy and energy density of Cu₂O–Al (4.08 kJ/g and 20.8 kJ/cm³ vs 2.41 kJ/g and 12.7 kJ/cm³), these formulations yield the same adiabatic flame temperature of 2843 K, which is dictated by the boiling point of Cu.¹² Major equilibrium products for both are liquid Al₂O₃ and Cu, along with gas-phase Cu. In the case of CuO–Al, the higher energy density allows for a much larger fraction of Cu to be vaporized. This difference in equilibrium gas production is the only significant difference between the two systems, thermodynamically.

While equilibrium calculations are useful to give us some idea of the final temperature, pressure, and composition, it has become more apparent recently that gaseous intermediate species may play a more dominant role in governing ignition and reaction processes.^{13–15} In particular, CuO is predicted to undergo decomposition to Cu₂O and release O₂ at a relatively low temperature, with the onset temperature generally shifting to lesser values as the atmospheric pressure decreases. Using time-resolved mass spectrometry, we have shown that rapidly heated (>10⁵ K/s) nanoparticles of CuO release O₂ at approximately 975 K.^{16,17} Cu₂O can further decompose to Cu and additional O₂, but this will occur at a higher temperature according to thermodynamic predictions. Therefore, a second significant difference between the two materials is that CuO has a low temperature gas-generation event as it decomposes into Cu₂O and liberates O₂ gas. What, exactly, is the benefit of this gas-generation step to ignition and combustion processes is a main question being addressed in this work. Furthermore, we are interested in what, if any, role does the size of the metal oxide play in contributing to the dynamic O₂ release.

To that end, CuO and Cu₂O particle sizes between 30 nm and 5 μm were mixed with nanometric aluminum. The ignition and transient O₂ release profiles were investigated in these materials at high heating rates using a combination of time-of-flight mass spectrometry (ToF-MS) and high-speed video at both atmospheric and vacuum conditions. Pressurization and optical measurements were performed using a constant volume combustion cell to characterize combustion behavior.¹³

■ EXPERIMENTAL METHODS

Materials. Cu₂O was synthesized using a method by Huang et al. that was scaled up to produce a larger quantity.¹¹ A 1 L volume, glass reaction vessel with a heating jacket set at 33.5 °C was used to heat and stir 860 mL of milli-Q water (18.2 MΩ) and 5 g of sodium dodecyl sulfate (OmniPur by VWR). A 20 mL volume of 0.1 M copper(II) chloride anhydrous (99% by Acros Organics) was then added to the solution. A 9 mL volume of 1 M sodium hydroxide (VWR) was subsequently added at which point the solution turned a light blue hue, indicating the formation of copper(II) hydroxide. After approximately 1 min, 80 mL of 0.1 M hydroxylamine hydrochloride (99% by Alfa Aesar) was added to the reaction vessel. The stirring (via magnetic stir bar) was stopped, and the Cu₂O particles were kept in the heated reaction vessel and allowed to grow for 1 h. After the 1 h growth process, the Cu₂O

particle solution was poured into four large (500 mL each) centrifuge tubes. The particle solution was centrifuged (Sorvall GS-3) at 9000 rpm for 15 min. The supernatant was removed and replaced with ethanol, and the Cu₂O particle pellet was resuspended using sonication and vortex mixing. This cleaning process was repeated three times. Organics remaining from the synthesis process made up ~5% of the final weight of the material as determined by thermogravimetric analysis (TGA). The different sizes of Cu₂O nanoparticles (ranging from 200 to 1500 nm) were obtained using the same synthesis recipe. Slight variation in the rate of the hydroxylamine hydrochloride addition and stirring during this process had a profound effect on the resulting Cu₂O size. SDS concentration and pH are other parameters that can be adjusted for size control.

CuO was produced from the synthesized Cu₂O through oxidation, by holding the material at 250 °C in air for 2 h. Conversion was confirmed through X-ray diffraction (XRD) and accompanied by a distinct color change from orange to black. Example XRD patterns are shown in the [Supporting Information](#), Figure S1.

Aluminum nanoparticles (Al-NPs) of average size 50 nm were used as purchased from Argonide Corp. They were considered 70% active by mass as a result of an ~3 nm native oxide shell. CuO was purchased from Sigma-Aldrich as a nanopowder (<50 nm primary particle size) and micrometer scale powder (<5 μm). Additional Cu nanopowder (60–80 nm) was also purchased from Sigma-Aldrich for use as a diluent.

Thermite mixtures were prepared stoichiometrically accounting for the oxide shell but not the organics on the Cu₂O. The samples were mixed with ultrasonication in hexane.

Characterization. Oxygen release and ignition were studied with temperature jump (T-jump) wire heating capable of rates of ~3 × 10⁵ K/s. Material was deposited from solvent suspensions onto thin (76 μm) platinum wires that were resistively heated with 3 ms electrical pulses. By measuring the current and voltage of the wire during the pulse, the temperature was calculated based on a well-known relationship for platinum resistance.¹⁸ Oxygen release was analyzed with a time-of-flight mass spectrometer (ToF-MS) that recorded spectra every 100 μs. Details of this experimental setup can be found in previous papers.^{16,17,19} Ignition was monitored with a high speed camera (Phantom v12.0, 67 000 frames per second) in both the ToF-MS and a chamber that was used for argon environment experiments. In such experiments, the chamber was evacuated with a mechanical pump, purged with argon flow, and then closed off to maintain 1 atm of argon.

Reactivity was quantified by igniting 25 mg of material in a constant volume (13 cm³) combustion cell capable of simultaneous optical and pressure measurements, the details of which can be found in a previous publication.¹³ At least two runs were performed for each material.

■ RESULTS

Examples of the synthesized Cu₂O nanoparticles are shown in [Figure 1a–d](#). As can be seen, the synthesis produced fairly monodisperse material over a wide range of sizes. Diameter was measured from scanning electron microscope (SEM) images and was found to vary by <10% for primary particles. The smaller particles tended to have less spherical morphologies in a manner consistent with previous studies of this synthesis method.¹¹ [Figure 1e,f](#) shows the CuO that resulted from oxidation of the material shown in [Figure 1a,b](#), respectively.

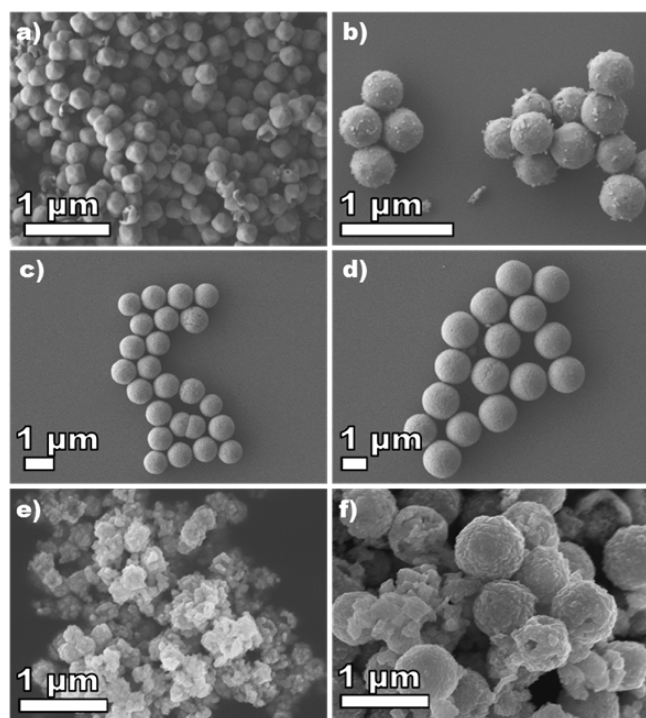


Figure 1. Scanning electron microscope (SEM) images of Cu_2O (a–d) synthesized for this study and the CuO (e, f) produced by oxidizing the material. The average Cu_2O particle diameters as determined from SEM analysis were 200, 390, 850, and 1510 nm for (a), (b), (c), and (d), respectively. Images in (e) and (f) are the results of oxidation (250 °C in air for 2 h) of the material shown in (a) and (b), respectively.

While many particles remained approximately the same size through oxidation, there was also significant morphological change that produced high surface roughness and some smaller irregularly shaped particles. As a result, the specific surface area increased during the oxidation, with 360 nm particles going from a BET surface area of 4.8 m^2/g to 6.9 m^2/g . It should also be noted that this specific surface area measured for the Cu_2O particles was ~ 1.7 times what would be expected for perfect spheres of that size, which can be accounted for by the surface roughness and malformed smaller particles visible in Figure 1a,b.

As mentioned above, CuO and Cu_2O have significantly different decomposition behaviors, which control how they release gaseous oxygen. Equilibrium calculations done with CHEETAH 6.0²⁰ and the JCZS library^{6,21} at 5×10^{-9} atm (approximately the vacuum of the mass spectrometer) predict that CuO will decompose into Cu_2O and O_2 at 800 K and that Cu_2O will decompose into Cu and O_2 at 1150 K. This behavior was studied experimentally using the T-jump ToF-MS at heating rates of $\sim 3 \times 10^5$ K/s. Along with the expected O_2 peak, significant H_2O and CO_2 peaks were also observed in the mass spectra for these materials, which suggests the presence of surface contamination for all (both commercial and synthesized) oxides used. Given that this is expected to be just a thin surface coating that should decompose at low temperatures, the potential impact of any hydrocarbons was largely ignored as is consistent with previous studies.^{17,19} Representative temporal O_2 species intensities are shown for both oxides and the corresponding thermites in Figure 2. Outside of expected experimental

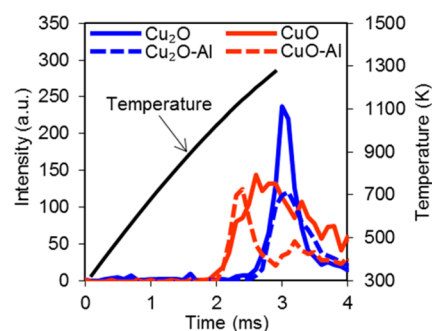


Figure 2. Example O_2 release profiles for the different oxides along with the corresponding thermite. The Cu_2O had a diameter of 320 nm, and the CuO was the oxidized version of that material. All samples were heated with temperature ramps ($\sim 3 \times 10^5$ K/s) similar to the black line shown. The points of O_2 release (defined at $>5\%$ of maximum) were 1050 and 1170 K for the CuO and Cu_2O , respectively, in this particular experiment.

variation, the general shapes of the O_2 profiles were consistent with the one shown in Figure 2 for all sizes of Cu_2O . This consistency is shown in Figure S2 of the Supporting Information along with the aforementioned H_2O and CO_2 profiles. From the oxygen profiles and corresponding temperature measurements, the O_2 release temperature is defined as the wire temperature measurement at the time when the signal intensity reaches $>5\%$ of the maximum and is employed to mark the onset of oxygen release. In these particular experimental runs, for CuO this point was 1050 K and for Cu_2O it was 1170 K. This difference is not as significant as predicted by the equilibrium calculations, which points to the fact that we are exploring kinetically limited processes as has previously been reported for CuO at high heating rates.¹⁹

Along with the O_2 release temperature, high speed video was used to record the reaction of the thermites. This allowed for the determination of an ignition temperature as defined by the onset of optical emission. However, the Cu_2O –Al reaction was found to be only weakly reactive in the vacuum of the mass spectrometer, making it difficult to distinguish the onset of reaction, but when heated under 1 atm of argon, it was found to be far more reactive. This difference is shown in Figure 3, where the integrated optical intensity from each video frame is plotted versus time with the background intensities of the blank wires (taken by pulsing the wires a second time) subtracted out.

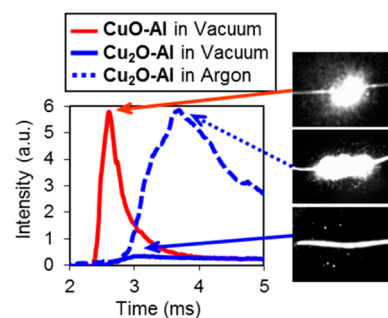


Figure 3. Integrated intensity of CuO –Al (commercial nanooxidizer, shown in red) and Cu_2O –Al (440 nm sized oxidizer, shown in blue) reaction in a vacuum (solid lines) and in argon (dashed line). Data is normalized by the peak intensity of a background run of the same wire used in the experiment, which is then subtracted out. Also shown are frames from the video corresponding to the peak visible reaction.

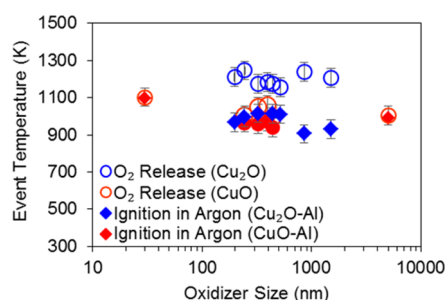


Figure 4. Oxygen release and ignition temperatures for the range of sizes tested. O_2 release temperature is defined at 5% of maximum, and ignition is defined by onset of optical emission from thermite. The unfilled circles represent the O_2 release from the oxidizer, and the filled diamonds are ignition in with Al-NPs in argon. The blue symbols are for Cu_2O , and the red symbols are for CuO . Note the logarithmic length scale.

Values are normalized to the peak value of the background run. The frames with peak intensity are also shown for reference. Figure 3 also includes the integrated intensity of CuO –Al reaction in a vacuum, which shows that it was able to achieve fast and intense reaction even in the mass spectrometer.

The measured oxygen release temperatures of neat CuO and Cu_2O are plotted along with the ignition temperature of the corresponding thermite in argon in Figure 4, as a function of oxidizer particle size. Each data point represents the average of at least two runs. The maximum run to run variation observed for onset temperatures was ± 50 K from the average. Accordingly, this value was used as a reasonable estimate for the error bars of all the data. For convenience, the size of the synthesized CuO samples was taken to be that of the precursor Cu_2O before conversion to CuO , although, as we discussed earlier, this does not necessarily reflect the actual size as oxidation led to significant changes in both size and morphology (see Figure 1). As can be seen in Figure 4, all of the CuO materials (red symbols) have consistent ignition temperatures (filled diamonds) within 100 K of the corresponding O_2 release temperatures (unfilled circles). In comparison, Cu_2O (blue symbols) thermites ignited ~ 200 K before the oxide released O_2 . Taking an average over all sizes, CuO and Cu_2O released oxygen at 1020 and 1200 K respectively, while with Al-NPs CuO and Cu_2O ignited at 970 and 980 K respectively. Another interesting feature of note is that there is no apparent size dependence on either O_2 release temperature or ignition temperature. Thus, it seems that the initiation of these processes is not limited by total specific surface area for the studied range of particle sizes.

Combustion results from the constant-volume pressure cell experiments are shown for Al mixed with commercial CuO (30 nm and $< 5 \mu m$) and synthesized 850 nm Cu_2O in Figure 5. The results show that CuO –Al was generally orders of magnitude more reactive than Cu_2O –Al. As can be seen for both pressure and optical signals, the nano CuO was the fastest material, with the micrometer CuO being about 2 orders of magnitude slower and the Cu_2O being an order of magnitude slower than that. Five different sizes of Cu_2O (190, 250, 390, 850, and 1500 nm) were tested, and all showed similar behavior to the 850 nm sample shown in Figure 5. In particular, the run to run variation was more significant than sample to sample, suggesting that there is no significant size dependence for Cu_2O from 200 to 1500 nm as is shown in the Supporting Information, Figures S3 and S4. The synthesized CuO (from

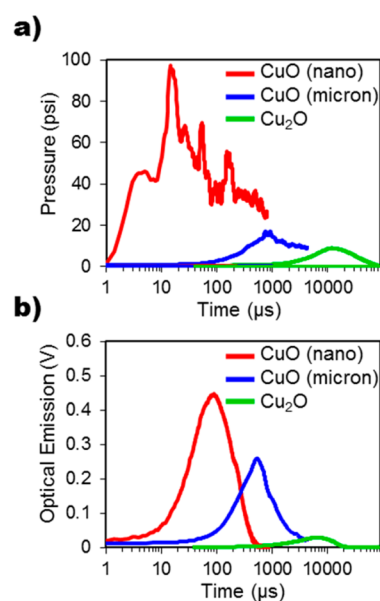


Figure 5. Results from reacting Al-NPs with the various oxidizers in a constant volume combustion cell. (a) Pressure response; (b) optical emission. Note the logarithmic scale of the x-axis. Nano CuO and micrometer CuO refer to the commercial material with primary sizes of 30 nm and $5 \mu m$, respectively.

oxidation of Cu_2O) of the sizes tested (original sizes 320 and 440 nm) performed nearly identically to the commercial nano CuO (< 50 nm) in terms of peak pressure and rise time, although there were noticeable features in the optical signal at later times. This can likely be attributed to the range of sizes that resulted from oxidation (see Figure 1e,f), with the smaller material accounting for the fast pressurization and the larger material reacting and emitting at later times.

To quantify these differences in reactivity, we look at the peak pressure, pressure rise time (i.e., time to peak pressure), and burning time (full width at half-maximum of optical signal). All of these values, as well as the key results from the T-jump experiments, are summarized in Table 1. Since there was no observable size dependence, the Cu_2O values are averaged together. We observed a significant drop in peak pressure moving from nano to micrometer CuO (from 110 to 20 psi), and a further reduction when using Cu_2O , which had a peak pressure of 8 psi. In terms of burning time, nano CuO and synthesized CuO were approximately the same, with micrometer CuO lagging behind. Cu_2O , in all cases, was dramatically slower than all CuO samples.

DISCUSSION

There are several interesting findings in this work that can be summed up as follows:

(a) Cu_2O –Al thermite ignites at exactly the same temperature as CuO –Al, despite its O_2 release temperature being approximately 200 K higher and the fact that it is at a lower oxidation state.

(b) There is no scaling of ignition temperature or oxygen release behavior with oxidizer particle size between 30 nm and $5 \mu m$. For Cu_2O –Al, there is no size dependence on reactivity of either, which is in stark contrast to CuO –Al.

(c) Cu_2O –Al thermites reacted poorly under vacuum and more violently at atmospheric pressure in argon.

Table 1. Quantified Results of the Different Experiments with Al-NPs and the Various Forms of Oxidizer

	T-jump experiments		combustion cell experiments		
	O ₂ release temp (K)	ignition temp (K)	peak press. (psi)	press. rise time (ms)	burning time (ms)
nano CuO	1030 (±50)	990 (±50)	110 (±16)	0.012 (±0.002)	0.28 (±0.1)
synthesized CuO	1030 (±50)	960 (±50)	100 (±8)	0.019 (±0.006)	0.33 (±0.12)
micrometer CuO	1000 (±50)	990 (±50)	20 (±4)	0.75 (±0.1)	0.86 (±0.3)
Cu ₂ O (average)	1200 (±50)	980 (±50)	8 (±1)	12 (±2)	11 (±3)

(d) Nano CuO, both commercial and synthesized, is the strongest oxidizer. Micrometer sized CuO yields about 5 times less pressure and produces longer pressure rise time and burning time by factors of about 60 and 3, respectively. Cu₂O was the poorest oxidizer, with significantly reduced pressure and much longer pressure rise and burning times than even the micrometer CuO.

The first point is a clear indication that the ignition process occurs directly through the condensed phase without the need for gaseous oxygen. Further, previous studies have found that Al-NPs thermite ignition is highly dependent on oxidizer, with ignition temperatures ranging from ~850 K (Bi₂O₃, MoO₃) to 1410 K (Fe₂O₃).¹⁶ This suggests that ignition is not primarily controlled by properties inherent to the Al, such as morphology or transport through the Al₂O₃ layer that exists natively and grows during reaction. Thus, the shared ignition temperatures of CuO and Cu₂O are indicative of shared mechanisms and controlling properties. Given the proximity of ignition and O₂ release for CuO–Al, it is possible that the primary interfacial reaction is between Al and the reduced form of CuO (i.e., Cu₂O) rather than CuO itself, which would explain the similar ignition temperatures of the two oxidizers. Such behavior was observed with in situ dynamic transmission electron microscopy (DTEM) experiments, where reaction proceeded only after decomposition of CuO.²² Whether this truly occurs during full scale reaction, and to what extent, would depend on the decomposition rate and time scale of liberating O₂ from the oxidizer relative to the interfacial reaction time scale, which are properties that have not been sufficiently characterized in order to definitively answer this question. In concert it should be noted that the heats of formation of CuO and Cu₂O are –156 and –170 kJ/mol, respectively. In other words, at least from a thermochemical standpoint the removal energy is roughly the same, which would suggest a similar ignition temperature, but shifted to slightly to account for the extra heat capacity of an additional Cu atom in Cu₂O.

The lack of a size dependence for ignition with CuO and Cu₂O is a very interesting finding and seemingly goes against previous results that showed ignition temperature is directly related to the amount of interfacial area in Al/CuO nanolaminates.²³ However, unlike the straightforward laminar structure of those materials, the relationship between the size of the components and interfacial area is not as clear-cut for nanoparticles. Spherical particles are limited to only small amounts of interfacial contact compared to their total surface area, and the complex aggregation that occurs in nanoparticles will further limit the amount of area in contact. Additionally, it has been shown that both Al and CuO nanoparticle aggregates will coalesce in <100 ns upon rapid (~10¹¹ K/s) heating.^{22,24} While typical combustion may not reach these extreme heating rates, this shows that loss of nanostructure can occur much faster than the other time scales found for combustion. Therefore, the actual size of the particles during the initial stages of reaction could be significantly larger than their starting

size. For all these reasons, the initial size of the oxidizer may not have as big an impact on fuel/oxidizer interfacial area as might be expected.

While ignition temperature was constant for both oxidizers through the range of sizes, the overall reactivity exhibited markedly different trends. As shown in Figure 5 and Table 1, the pressure rise time for CuO–Al increased by a factor of ~50 as the oxidizer size was increased from nanometers to micrometers. This is consistent with a previous study by Weismiller et al. that found the length scale of the oxidizer to be one of the most critical factors in determining reactivity.¹ In contrast, Cu₂O–Al exhibited no significant size dependence from 200 nm to 1.5 μm as discussed above and shown in Figures S3 and S4 in the Supporting Information. This suggests that the Cu₂O–Al combustion is limited by some property that is weakly or not at all size dependent. One possibility is that it is heat transport limited. Due to the small amount of gas produced, the typical convective/advective mode may not be accessible and instead conduction could dominate.^{7–10} While the size of the particles could affect conduction, aluminum has a much higher thermal conductivity and is the same size in all cases, which could minimize the impact of this effect.

The observation that Cu₂O did not react nearly as well under vacuum as it did at atmospheric pressure suggests that the gases liberated during combustion play an important role in determining overall reactivity, even if they do not initiate ignition. Given that both oxidizers have been shown to release O₂ during reaction, it follows that secondary oxidation with intermediate O₂ could be a significant pathway for reaction, but one that would be significantly diminished under vacuum conditions where gases can rapidly diffuse away from the reaction zone. In comparison to the lower oxidation state oxide, Figure 3 shows that CuO can react violently even in a vacuum, which suggests that it can produce O₂ fast enough to sustain a localized oxidizing environment. However, as with Cu₂O–Al, the reaction of CuO–Al is enhanced by the presence of an argon environment, which causes the reaction to be much brighter and to last longer as is shown in the Supporting Information with Figure S5. This is further evidence that localizing the produced gases enhances reactions and points toward a slower (on the order of ~2 ms) secondary reaction with gaseous oxygen that accounts for a significant portion of the overall energy release. The general process of fast O₂ release followed by heterogeneous reaction has been previously supported for nano CuO–Al based on the sharp pressure rise that precedes the peak of the optical signal in combustion cell experiment as well as the long (~3 ms) burning that occurs well after the initial fast flame front has passed in burn tubes.^{13–15}

The faster and more significant O₂ release that allowed CuO–Al to react violently in a vacuum could also explain, in part, the final point above about the poor pressure cell performance of the Cu₂O–Al. Beyond serving as a secondary oxidizer, this gas could play other critical roles in combustion,

particularly with regard to heat transfer, which is generally thought to be controlled by large pressure gradients driving hot gases and condensed phase material forward into the unreacted zone.^{7–9} Strong gas generation could also potentially offset the growth of large clusters, which would preserve some of the high surface area and allow for faster reaction in the later stages of combustion. Previous observations made with phase contrast imaging for both CuO–Al (strong gas generator) and Fe₂O₃ thermites (weak gas generator) indicated that the CuO–Al system yielded significantly smaller material being ejected from the wire.²⁵ Additionally, we have recently shown that the use of nitrocellulose as a gas generator and structural component can significantly assist thermite combustion by acting as a dispersant and reducing coalescence and sintering.²⁶

These nonoxidizing roles may also be filled by the primary product gas, Cu, as well as by the intermediate O₂. As Cu is also greatly diminished for the Cu₂O–Al case, it is important to consider that this may also be a reason for the thermite's poor pressure cell performance. In order to get a rough measure of the importance of each gas, we also tested a CuO–Al system diluted with Cu ($3\text{Cu} + 3\text{CuO} + 2\text{Al} \rightarrow 6\text{Cu} + \text{Al}_2\text{O}_3$) in a way that simulates the thermodynamics of the Cu₂O–Al system ($3\text{Cu}_2\text{O} + 2\text{Al} \rightarrow 6\text{Cu} + \text{Al}_2\text{O}_3$). For this CuO–Cu–Al system, the oxidizer will decompose to release O₂ in the same manner as the CuO–Al case, but will produce Cu vapor at levels closer to Cu₂O–Al. Constant pressure (1 atm) equilibrium calculations indicate that CuO–Cu–Al and Cu₂O–Al systems will produce 0.54 and 0.27 mol of product Cu vapor per kilogram of reactant respectively in contrast to the 3.7 mol/kg produced by CuO–Al. Thus, a poor pressure cell performance of the diluted system will indicate that Cu vapor is very important to combustion, while performance comparable to CuO–Al will support intermediate O₂ being the critical gas.

Experimentally we found the Cu–CuO–Al system (commercial 30 nm CuO and 60–80 nm Cu) performed almost identically to the micrometer CuO–Al case (both are plotted in the Supporting Information, Figure S6) with a peak pressure of 17 psi, a pressure rise time of 0.86 ms, and a burning time of 0.74 ms. That these line up so well indicates that both systems are limited by the same process. This could be the O₂ release rate, as CuO–Cu will release less O₂ on a per mass basis and micrometer CuO could be slowed by longer transport times of oxygen anion through the larger particles.²⁷ Both could also be limited by condensed phase kinetics, with the Cu particles blocking access of the fuel to oxidizer in the same way large oxidizer particles shut out the internal oxidizer in the early stages of reaction. Regardless, the key finding is that CuO–Cu–Al outperforms Cu₂O–Al by an order of magnitude despite sharing very similar equilibrium gas production. Thus, the intermediate O₂ plays a more significant role in the overall combustion process. This gas, released vigorously from CuO relative to Cu₂O and in the early stages of reaction, likely serves as a key driver in heat transfer by providing a source of pressurization to push hot material into the unreacted zone. This is in comparison to Cu gas, which is only produced as the last step of the reaction once the material has already reached the adiabatic flame temperature, which is the boiling point of copper vapor (2835 K).

Combining all these results and discussions, we can develop a theory of the overall combustion process for copper oxide based nanocomposite thermites. From both oxides igniting at the same temperature and before O₂ release in Cu₂O, the ignition process occurs through a condensed phase reaction.

Such a mechanism has been shown to potentially occur very quickly once the reactants are mobile, so this would quickly release significant energy.²² The energy would raise the local temperature of the material and drive the decomposition of the unreacted oxidizer to produce O₂, most efficiently from CuO, which produces a pressure gradient that drives hot material forward to the unreacted zone and thereby propagates the reaction. Additionally, it provides a secondary oxidizer to sustain the reaction and move it toward completion. Some Cu vapor will also be produced during the reaction that will further support the heat transfer aspect, but to a lesser degree than the intermediate gas.

CONCLUSION

The ignition and reaction properties of aluminum nanocomposite thermites with copper oxide oxidizers were studied with a variety of experiments. Monodisperse Cu₂O was synthesized in sizes ranging from 200 to 1500 nm and tested with temperature jump (T-jump) heating of $>10^5$ K/s for oxygen release and ignition with nanoaluminum. These results were compared with CuO systems which have many similar properties but produce more intermediate (O₂) and equilibrium (Cu) gas. Cu₂O was found to release oxygen around 200 K higher than CuO, but ignite at the same temperature as the other oxidizer. This suggests that both oxides ignite through a condensed phase mechanism independent of gaseous oxygen. Cu₂O–Al reacted only very weakly in the vacuum environment and significantly more strongly in argon, which implies that secondary heterogeneous oxidation from O₂ is important for sustaining strong reaction.

Reactivity tests in a constant volume combustion cell showed that Cu₂O–Al thermites performed similarly, independent of oxidizer size and were ~ 3 orders of magnitude slower than nano CuO thermites and ~ 1 order of magnitude slower than micrometer CuO thermite. CuO–Cu–Al was also tested as it has the intermediate gas release properties of CuO, with the equilibrium gases of Cu₂O–Al. The diluted system performed the same as micrometer CuO, which implies that O₂ production plays a significant role in both reaction and heat transfer.

ASSOCIATED CONTENT

Supporting Information

The Supporting Information is available free of charge on the ACS Publications website at DOI: 10.1021/acs.jpcc.6b11081.

Comparison of X-ray diffraction (XRD) patterns for Cu₂O nanoparticles before and after conversion to CuO; example mass spectrometer results from Cu₂O NPs of different sizes; combustion cell results for Cu₂O–Al; difference in optical intensity from T-jump CuO–Al experiments in vacuum and argon; combustion cell results from CuO–Cu–Al experiment (PDF)

AUTHOR INFORMATION

Corresponding Author

*E-mail: mrz@umd.edu.

ORCID

Michael R. Zachariah: 0000-0002-4115-3324

Present Address

[§]G.C.E.: Materials Science Division, Lawrence Livermore National Laboratory, Livermore, CA 94550, USA.

Notes

The authors declare no competing financial interest.

ACKNOWLEDGMENTS

We acknowledge the help of Pui Ching (Steve) Lan in synthesizing the Cu₂O nanoparticles. Work conducted by M.R.Z. and G.C.E. has been supported by the Army Research Office (Ralph Anthenien) and the Defense Threat Reduction Agency. Work conducted by K.T.S., T.Y.O., M.A.W., and T.Y.-J.H. was supported by the Laboratory Directed Research and Development Program at LLNL (13-ER-022, 14-SI-004). This work was performed under the auspices of the U.S. Department of Energy by Lawrence Livermore National Laboratory under Contract No. DE-AC52-07NA27344. This paper was reviewed for release as LLNL-JRNL-681429.

REFERENCES

- (1) Weismiller, M. R.; Malchi, J. Y.; Lee, J. G.; Yetter, R. A.; Foley, T. J. Effects of Fuel and Oxidizer Particle Dimensions on the Propagation of Aluminum Containing Thermites. *Proc. Combust. Inst.* **2011**, *33*, 1989–1996.
- (2) Asay, B. W.; Son, S. E.; Busse, J. R.; Oschwald, D. M. Ignition Characteristics of Metastable Intermolecular Composites. *Propellants, Explos., Pyrotech.* **2004**, *29*, 216–219.
- (3) Bockmon, B. S.; Pantoya, M. L.; Son, S. F.; Asay, B. W.; Mang, J. T. Combustion Velocities and Propagation Mechanisms of Metastable Interstitial Composites. *J. Appl. Phys.* **2005**, *98*, 064903.
- (4) Dutro, G.; Son, S.; Tappan, A. The Effect of Microscale Confinement Diameter on the Combustion of an Al/MoO₃ Thermite. Presented at the 44th AIAA/ASME/SAE/ASEE Joint Propulsion Conference & Exhibit, 2008.
- (5) Pantoya, M. L.; Granier, J. J. Combustion Behavior of Highly Energetic Thermites: Nano Versus Micron Composites. *Propellants, Explos., Pyrotech.* **2005**, *30*, 53–62.
- (6) Sanders, V. E.; Asay, B. W.; Foley, T. J.; Tappan, B. C.; Pacheco, A. N.; Son, S. F. Reaction Propagation of Four Nanoscale Energetic Composites (Al/MoO₃, Al/Wo₃, Al/Cuo, and Bi₂O₃). *J. Propul. Power* **2007**, *23*, 707–714.
- (7) Weismiller, M. R.; Malchi, J. Y.; Yetter, R. A.; Foley, T. J. Dependence of Flame Propagation on Pressure and Pressurizing Gas for an Al/Cuo Nanoscale Thermite. *Proc. Combust. Inst.* **2009**, *32*, 1895–1903.
- (8) Egan, G. C.; Zachariah, M. R. Commentary on the Heat Transfer Mechanisms Controlling Propagation in Nanothermites. *Combust. Flame* **2015**, *162*, 2959–2961.
- (9) Son, S. F.; Asay, B. W.; Foley, T. J.; Yetter, R. A.; Wu, M. H.; Risha, G. A. Combustion of Nanoscale Al/Moo₃ Thermite in Microchannels. *J. Propul. Power* **2007**, *23*, 715–721.
- (10) Sullivan, K. T.; Kuntz, J. D.; Gash, A. E. Electrophoretic Deposition and Mechanistic Studies of Nano-Al/Cuo Thermites. *J. Appl. Phys.* **2012**, *112*, 024316.
- (11) Huang, W.-C.; Lyu, L.-M.; Yang, Y.-C.; Huang, M. H. Synthesis of Cu₂O Nanocrystals from Cubic to Rhombic Dodecahedral Structures and Their Comparative Photocatalytic Activity. *J. Am. Chem. Soc.* **2012**, *134*, 1261–1267.
- (12) Fischer, S. H.; Grubelich, M. C., A Survey of Combustible Metals, Thermites, and Intermetallics for Pyrotechnic applications. In *32nd AIAA/ASME/SAE/ASEE Joint Propulsion Conference*; Sandia National Laboratories: Lake Buena Vista, FL, 1996.
- (13) Sullivan, K.; Zachariah, M. R. Simultaneous Pressure and Optical Measurements of Nanoaluminum Thermites: Investigating the Reaction Mechanism. *J. Propul. Power* **2010**, *26*, 467–472.
- (14) Densmore, J. M.; Sullivan, K. T.; Gash, A. E.; Kuntz, J. D. Expansion Behavior and Temperature Mapping of Thermites in Burn Tubes as a Function of Fill Length. *Propellants, Explos., Pyrotech.* **2014**, *39*, 416–422.
- (15) Sullivan, K. T.; Cervantes, O.; Densmore, J. M.; Kuntz, J. D.; Gash, A. E.; Molitoris, J. D. Quantifying Dynamic Processes in Reactive Materials: An Extended Burn Tube Test. *Propellants, Explos., Pyrotech.* **2015**, *40*, 394–401.
- (16) Jian, G.; Chowdhury, S.; Sullivan, K.; Zachariah, M. R. Nanothermite Reactions: Is Gas Phase Oxygen Generation from the Oxygen Carrier an Essential Prerequisite to Ignition? *Combust. Flame* **2013**, *160*, 432–437.
- (17) Zhou, L.; Piekiet, N.; Chowdhury, S.; Zachariah, M. R. Time-Resolved Mass Spectrometry of the Exothermic Reaction between Nanoaluminum and Metal Oxides: The Role of Oxygen Release. *J. Phys. Chem. C* **2010**, *114*, 14269–14275.
- (18) Preston-Thomas, H. The International Temperature Scale of 1990(Its-90). *Metrologia* **1990**, *27*, 3–10.
- (19) Jian, G.; Piekiet, N. W.; Zachariah, M. R. Time-Resolved Mass Spectrometry of Nano-Al and Nano-Al/Cuo Thermite under Rapid Heating: A Mechanistic Study. *J. Phys. Chem. C* **2012**, *116*, 26881–26887.
- (20) Bastea, S.; Fried, L.; Glaesemann, K.; Howard, W.; Kuo, I.; Souers, P.; Vitello, P. *CHEETAH 6.0. User's Manual*; Lawrence Livermore National Laboratory: 2010.
- (21) Hobbs, M. L.; Baer, M. R.; McGee, B. C. Jc₂: An Intermolecular Potential Database for Performing Accurate Detonation and Expansion Calculations. *Propellants, Explos., Pyrotech.* **1999**, *24*, 269–279.
- (22) Egan, G. C.; LaGrange, T.; Zachariah, M. R. Time-Resolved Nanosecond Imaging of Nanoscale Condensed Phase Reaction. *J. Phys. Chem. C* **2015**, *119*, 2792–2797.
- (23) Egan, G. C.; Mily, E. J.; Maria, J. P.; Zachariah, M. R. Probing the Reaction Dynamics of Thermite Nanolaminates. *J. Phys. Chem. C* **2015**, *119*, 20401–20408.
- (24) Egan, G. C.; Sullivan, K. T.; LaGrange, T.; Reed, B. W.; Zachariah, M. R. In Situ Imaging of Ultra-Fast Loss of Nanostructure in Nanoparticle Aggregates. *J. Appl. Phys.* **2014**, *115*, 084903.
- (25) Sullivan, K. T.; Piekiet, N. W.; Wu, C.; Chowdhury, S.; Kelly, S. T.; Hufnagel, T. C.; Fezzaa, K.; Zachariah, M. R. Reactive Sintering: An Important Component in the Combustion of Nanocomposite Thermites. *Combust. Flame* **2012**, *159*, 2–15.
- (26) Wang, H.; Jian, G.; Egan, G. C.; Zachariah, M. R. Assembly and Reactive Properties of Al/Cuo Based Nanothermite Microparticles. *Combust. Flame* **2014**, *161*, 2203–2208.
- (27) Jian, G.; Zhou, L.; Piekiet, N. W.; Zachariah, M. R. Low Effective Activation Energies for Oxygen Release from Metal Oxides: Evidence for Mass-Transfer Limits at High Heating Rates. *ChemPhysChem* **2014**, *15*, 1666–1672.